Metallomics

Accepted Manuscript

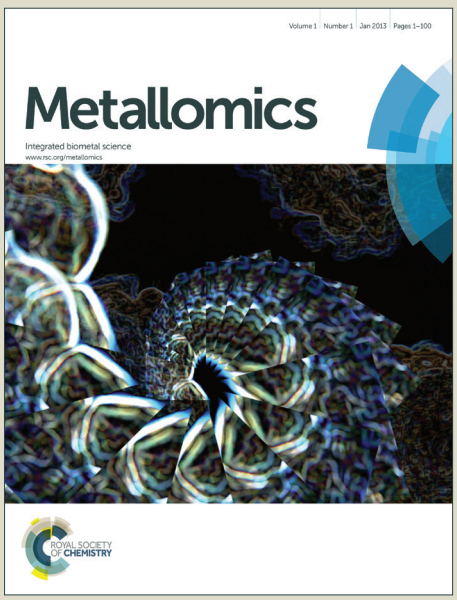

ROYAL SOCIETY OF CHEMISTRY

www.rsc.org/metallomics

The early plant root response to uranyl was characterized using complete Arabidopsis transcriptome microarrays. Hypotheses are presented to explain how uranyl perturbs the expression of genes coding the main actors involved in iron uptake and signaling (IRT1, FRO2, AHA2, AHA7 and FIT1) in plants.

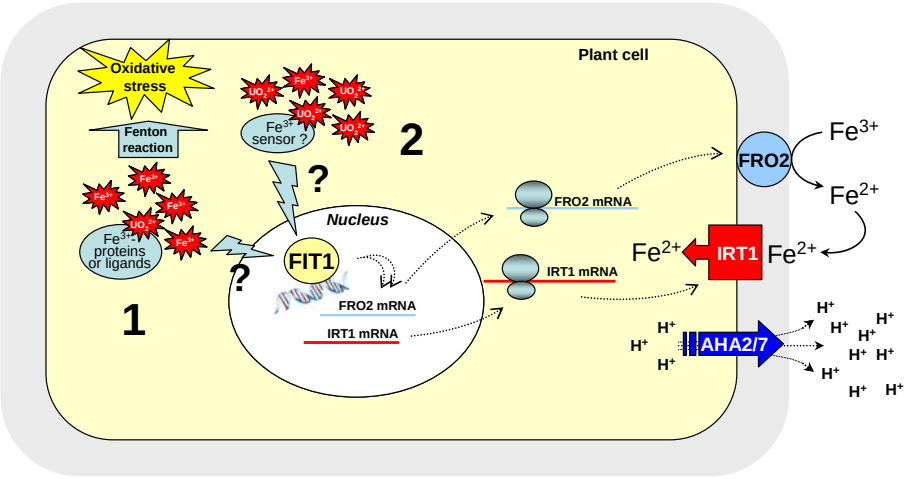

Uranium perturbs signaling and iron uptake response in *Arabidopsis thaliana* roots

Fany Doustaly[1,2,3,4], Florence Combes[2,5,6,*], Julie Fiévet[1,2,3,4*], Serge Berthet[1,2,3,4], Véronique Hugouvieux[1,2,3,4], Olivier Bastien[1,2,3,4], Iker Aranjuelo[1,2,3,4,7], Nathalie Leonhardt[8], Corinne Rivasseau[1,2,3,4], Marie Carrière[9], Alain Vavasseur[8], Jean-Pierre Renou[10,11], Yves Vandenbrouck[2,5,6] and Jacques Bourguignon[1,2,3,4]*

[1]Commissariat à l'Energie Atomique et aux Energies Alternatives (CEA), Direction des Sciences du Vivant (DSV), Institut de Recherche en Technologies et Sciences pour le Vivant (iRTSV), Laboratoire de Physiologie Cellulaire Végétale (PCV), Grenoble F-38054, France

[2]Univ. Grenoble Alpes, PCV, Grenoble F-38054, France.

[3]INRA (USC1359), PCV, Grenoble F-38054, France., France.

[4]CNRS (UMR 5168), PCV, Grenoble F-38054

[5]CEA, DSV, iRTSV, Laboratoire de Biologie à Grande Echelle, Grenoble F-38054, France.

[6] INSERM, Unité 1038, Grenoble F-38054, France.

[7] Instituto de Agrobiotecnología, Universidad Pública de Navarra-CSIC-Gobierno de Navarra, Campus de Arrosadía, E-31192-Mutilva Baja, Spain.

[8]CEA, CNRS, Université Aix-Marseille, Laboratoire de Biologie du Développement des Plantes, UMR 7265, St Paul lez-Durance, F-13108, France.

[9]CEA, INAC, UMR E3 CEA-UJF, SCIB, Laboratoire Lésions des Acides Nucléiques, F-38054 Grenoble, France.

[10]Unité de Recherche en Génomique Végétale, UMR1165, INRA, CNRS, Université d'Evry Val d'Essonne, 91057 Evry, France.

*These authors contributed equally to the work.

Footnotes:

Financial source

This work was funded by the CEA Toxicology Program. IA had a "Coopération et Mobilité Internationales Rhône Alpes » (CMIRA) grant from the Rhône-Alpes region.

[11]Present address: Institut de Recherche en Horticulture et Semences, INRA, Université d'Angers, 42, rue Georges Morel - BP 60057 - 49071 Beaucouzé Cedex – France.

Corresponding author: Jacques Bourguignon, CEA, Univ. Grenoble Alpes, CNRS, INRA, iRTSV, PCV, 17 rue des Martyrs, 38054 Grenoble cedex 9, France.

E-mail: jacques.bourguignon@cea.fr

SUMMARY

Uranium is a natural element which is mainly redistributed in the environment due to human activity, including accidents and spillages. Plants may be useful in cleaning up after incidents, although little is yet known about the relationship between metal speciation and plant response. Here, J-Chess modeling was used to predict U speciation and exposure conditions affecting U bioavailability for plants. The model was confirmed by exposing *Arabidopsis thaliana* plants to U in hydroponic conditions. The early root response was characterized using complete Arabidopsis transcriptome microarrays (CATMA). Expression of 111 genes was modified at the three timepoints studied. The associated biological processes were further examined by real-time quantitative RT-PCR. Annotation revealed oxidative stress, cell wall and hormone biosynthesis, and signaling pathways (including phosphate signaling) were affected by U exposure. The main actors in iron uptake and signaling (*IRT1*, *FRO2*, *AHA2*, *AHA7* and *FIT1*) were strongly down-regulated upon exposure to uranyl. A network calculated using *IRT1*, *FRO2* and *FIT1* as bait revealed a set of genes whose expression levels change under U stress. Hypotheses are presented to explain how U perturbs the iron uptake and signaling response. These results give preliminary insights into the pathways affected by uranyl uptake, which will be of interest for engineering plants to help clean areas contaminated with U.

Introduction

Uranium (U) is the heaviest existing natural element and has 23 radioactive isotopes; isotopes ^{238}U (99.27%), ^{235}U (0.72%) and ^{234}U (0.0055%) are the most abundant.[1] It is a naturally occurring radionuclide and metallic trace element, found at 2 to 5 $mg.kg^{-1}$, on average, in the earth's crust. In phosphate-containing rocks, it can be present at 20 to 150 $mg.kg^{-1}$. In the environment, U is mainly redistributed due to anthropogenic activities. The most contaminating industries are U mining and milling, metal mining and smelting, and the phosphate industry.[2] Agricultural phosphate fertilization is also a major source of U contamination,[3,4] with U at up to 700 mg of U / kg in Triple SuperPhosphate. The two major oxidation states are U (+VI) and U (+IV). U (+IV) can be oxidized to U (+VI) as UO_2^{2+}, the uranyl ion, which is the most stable U species in an oxidizing solution; it is therefore the most prevalent form found in the environment. As uranyl, U can form ion complexes with carbonate, phosphate or sulfate. In these forms, U is soluble and readily transported. In contrast, under reducing conditions, such as those found in anoxic water and sediment, U occurs in its tetravalent form (U (+IV)). In this state it has a strong tendency to bind to organic material and to precipitate, rendering it immobile.[5] As uranyl, U may be taken up by plants and, through them, can enter the food chain where it can exert both chemotoxic and radiotoxic effects. Radiological toxicity is directly related to the effects of ionizing radiation, thus only enriched U presents a radiological problem. In contrast, chemical toxicity is particularly significant in compounds containing natural U [6] (and references therein).

The chemical toxicity of U has been predominantly analyzed in humans and other animals but rarely in plants.[7-11] In *Phaseolus vulgaris*, U toxicity appears only at relatively high concentrations; concentrations of 0.1 to 1000 µM (in hydroponic conditions and for a 7-day treatment) did not significantly affect *P. vulgaris* growth.[7] As with other heavy metals, U may induce oxidative stress in plants, causing a cellular redox imbalance leading to a loss of DNA integrity at high concentrations (1 mM). In response to U, most of the enzymes involved in anti-oxidant defense mechanisms show slight dose-response stimulation in roots (with [U] ≤ 100 µM), but are not affected in primary leaves.[7] Over the same concentration range (≤ 100 µM), total and reduced glutathione (GSH) increased in leaves in exposed plants. At 1000 µM, GSH concentrations drop once again. In the treatment conditions described by Vandenhove *et al.* (2006), the U toxicity threshold seems to be between 100 and 1000 µM for *P. vulgaris*. The same group studied U exposure in *Arabidopsis thaliana*, and confirmed that the cellular redox balance is strongly disrupted during U stress at relatively high concentrations (100 µM).[8-11] At this concentration, enzymes involved in stress signaling and the oxidative stress response are over-expressed in roots. Among the enzymes affected, plasmalemmic NADPH-oxidase is up-regulated, suggesting a fast

oxidative burst. Simultaneously, an increase in lipoxygenase (*LOX1*) expression may enhance the production of signaling molecules such as jasmonate. Some defense enzymes involved in ROS scavenging, such as iron super oxide dismutase (*FSD1*), catalase (*CAT1*) and ascorbate peroxidase (*APX1*), are also up-regulated. However, this up-regulation is not sufficient to avoid a cellular redox imbalance.[8,10] Work on *Brassica napus* has also indicated a perturbed cellular GSH/GSSG balance in cells treated with U.[12]

Thus, the cellular and molecular responses to U stress in plants are poorly described. The cellular mechanisms involved in U detoxification, U-induced signal transduction pathways, and the mechanisms by which U modulates the expression levels of most genes remain unknown. Understanding these responses is essential if plants are to be engineered to clean up soils contaminated with U. This increased knowledge will also help avoid nutritional diseases by limiting toxic metal intake through the food chain.

The development of global 'omics' approaches has opened up the possibility of an in-depth exploration of cell function and regulation. These approaches have been useful in deciphering the plant response to heavy metals.[13-19] Here, microarray technology was used to analyze the transcriptomic response to U stress in Arabidopsis roots. We first established the hydroponic treatment conditions and characterized the phenotype of metal-treated *Arabidopsis thaliana* plants. The early transcriptomic response in 7-week-old plants was then analyzed after treatment with uranyl nitrate for different times. CATMA microarray results were confirmed and completed by real-time quantitative RT-PCR (qRT-PCR) experiments and the biological processes affected by U were fully characterized. To gain further insights into the underlying transcriptional network invoked by this abiotic stress, co-expression analysis was performed using a guide-gene approach. These results combined allow us to suggest a new gene-to-gene relationship in the iron regulatory network which is perturbed by U. Hypotheses are presented that could explain how uranyl affects the root iron-uptake and signaling response.

Experimental

Plant materials and uranium treatments

Arabidopsis thaliana plants, ecotype Columbia, were grown hydroponically in a controlled environment with an 8-h light period at 22 °C (~ 110 µmol $m^{-2}s^{-1}$) followed by a 16-h dark period at 20 °C. Relative humidity was maintained at 65%. A nutritive solution was supplied, composed of: 805 µM $Ca(NO_3)_2$, 2 mM KNO_3, 60 µM K_2HPO_4, 695 µM KH_2PO_4, 1.1 µM $MgSO_4$, 20 µM $FeSO_4$, 20 µM Na_2EDTA, 74 nM $(NH_4)_6Mo_7O_{24}$, 3.6 µM $MnSO_4$, 3 µM $ZnSO_4$, 9.25 µM H_3BO_3, 785 nM $CuSO_4$, with a pH of 5.6. After 7 weeks' normal growth, plants were treated with U (uranyl nitrate hexahydrate, Fluka) prepared in water or in the nutritive solution for 2 to 96 h. Where indicated, water was supplemented with citrate (200 µM), or with a culture medium lacking EDTA and both forms of phosphate (K_2HPO_4 and KH_2PO_4). Before harvesting, roots were first rinsed with 10 mM Na_2CO_3, then with water, and finally dried on tissue paper. Roots and leaves were then cut, flash-frozen in liquid nitrogen and stored at -80 °C.

Microarray experiments

The roots from five plants per group were pooled (groups: untreated, treated with 50 µM uranyl for 2, 6 and 30 h). Total RNA was extracted using a QIAGEN RNeasy Plant Mini Kit according to the manufacturer's instructions. Two independent biological replicates were performed. The integrity of extracted RNA was verified (Agilent bioanalyzer). Microarray analyses were then performed using Complete Arabidopsis Transcriptome MicroArray (CATMA) chips. These chips contained 24,576 nuclear gene-specific tags (GST) for *Arabidopsis*, which correspond to 22,089 nuclear genes, including 21,612 AGI-predicted genes and 477 Eugene-predicted genes.[20,21] One technical replicate with fluorochrome reversal was performed to avoid dye bias. A gene-specific dye bias, dye-swap experiment was also performed for each comparison.[22] Reverse transcription of RNA in the presence of Cy3-dUTP or Cy5-dUTP (Perkin-Elmer-NEN Life Science Products), hybridization of labeled samples to the slides, and slide scanning were all performed as described in Herbette *et al.*[16]

Microarray data analysis

CATMA microarrays were normalized using the global-Locally weighted scatterplot smoothing (lowess) method with the Goulphar R-script.[23] Differential analysis was then performed with the Linear Models for Microarray Data (limma) package[24] from the Bioconductor project.[25] Differences in gene expression were considered statistically significant with a P-value < 0.001 (after a Benjamini-Hochberg correction procedure).[26] The complete dataset has been deposited in the CATdb repository (project name "CEA06-01_Uranyl_nitrate", http://urgv.evry.inra.fr/CATdb), and

in the GEO repository under accession number GSE11797 (http://www.ncbi.nlm.nih.gov/geo/).

Real-Time quantitative RT-PCR

Total RNA was extracted from samples using RNeasy Plant Mini Kit (Qiagen) according to the manufacturer's instructions. RNA integrity was gel-tested and quantified using a Nanodrop ® 2000 (Thermoscientific). Total RNA was treated with DNA-free Turbo DNAse (Ambion). Total RNA (1 µg) was used to synthesize cDNA with M-MLV Reverse Transcriptase RNase H Minus, Point Mutant (Promega), and olido dT primers in a total reaction volume of 20 µl. At the end of the reaction, 180 µl of water was added. Real-time RT-PCR reactions were performed with 5 µl diluted cDNA mixture, in triplicate, on a Rotor-Gene 3000 instrument (Corbett Research) using SYBR Green JumpStart Taq ReadyMix (Sigma-Aldrich). For each gene, specific primers (see Supplemental Table S1) were designed using Primer BLAST (http://www.ncbi.nlm.nih.gov). A series of 7 dilutions for each cDNA sample was used to establish standard curves. The actin2/7 gene (At5g09810) was used as control. Gene expression was quantified based on the $2^{-\Delta\Delta Ct}$ method.[27]

Chlorophyll and anthocyanin contents

Total chlorophyll concentration was determined by extraction with 80% acetone, according to Arnon[28]; total anthocyanins were determined according to Lange *et al.*[29]

Uranium and Fe quantification

For U and Fe measurements, shoots and roots (about 100 mg of fresh material) from treated and untreated plants were dried for 1 day at 80 °C. Samples were then mineralized in 5 mL of 65% (v/v) HNO_3 (Suprapur; Merck) and 1 mL of 30% (v/v) HCl (Suprapur, Merck) at 180 °C. After complete evaporation of the mixture, residual material was dissolved in 1% (v/v) HNO_3. U and Fe concentrations in the extract were finally determined by ICP-MS (HP4500 ChemStation ICP-MS device; Yokogawa Analytical Systems) measurement of ^{238}U and ^{57}Fe.

Predicting uranium speciation

Uranium speciation was modeled in various exposure media using the geochemical speciation Java Chemical Equilibrium with Species and Surfaces software (J-Chess version 3.0; http://chess.ensmp.fr). Input data was supplied by the Base Applied to Speciation in Solution at Interface and Solubility (BASSIST) database.[30] This thermodynamic database includes selected values from the International Nuclear Energy Agency and the Paul Scherrer Institute. These values can be updated, as recommended by Denison and Garnier-LaPlace,[31] by adding or modifying data concerning U-citrate complexes (for details see Laurette *et al.*, 2012b).

Co-expression analysis

The microarray data used for this part of the work was from two-color Arabidopsis CATMA microarrays. Projects were downloaded in January 2012 from the CATdb repository.[32] The resulting compendium consisted of 205 projects representing 1567 hybridized samples in a range of experimental conditions. The probes cover a total of 24,576 Arabidopsis genes. The raw data were normalized using the print-tip lowess normalization method in the limma package[33] from the Bioconductor project.[25] Co-expression was analyzed as detailed in Boyer *et al.*[34] We then applied the guide-gene strategy using a set of pre-selected genes, or bait genes.[35] From all co-expression graphs (one per project), genes that are direct neighbors of at least one of the chosen bait genes, and edges that (i) connect gene pairs with a corrected P-value ≤ 0.005 and (ii) exist in at least 3 co-expression graphs were selected to form a summary graph that we call a transcriptional module.

Results

Uranyl exposure conditions and phenotypic characterization of U-treated *Arabidopsis thaliana* plants

To determine the impact of U on plants grown in hydroponic conditions, the presence of U species in solution was predicted by thermodynamic calculation using J-Chess modeling software[36] and the radionuclide chemistry BASSIST database.[30] The predicted U speciation for 5, 50 and 200 µM uranyl nitrate in the culture medium or in water with respect to pH is presented in Figure 1. In the nutrient solution, due to the presence of phosphate, U at 50 and 200 µM was predicted to precipitate between pH 3.0 and 8.0 as $(UO_2)_3(PO_4)_2$•$6H_20$ and saleeite ($Mg(UO_2)_2(PO_4)_2$•$10(H_2O)$) complexes (Fig. 1A, B &C). At 5 µM uranyl, most U was also present in these two insoluble forms, but at lower pH (pH< 4) the following soluble forms appeared: UO_2HPO_4, UO_2^{2+}, $UO_2H_2PO_4^{+}$ and UO_2SO_4. For all concentrations in water at a pH between 2.5 and 4.5, calculations predict the predominant soluble form of U present to be the uranyl ion (UO_2^{2+}) (Fig. 1D, E & F). $UO_2(OH)^{+}$ should also be present in smaller proportions. At higher pH, the insoluble schoepite form ($(UO_2)_8O(OH)_{12}$•$12(H_2O)$) is the most abundant.

To test the relevance of these predictions in treatment conditions, Arabidopsis plants were grown for 7 weeks in the culture medium and then treated with 0, 50 or 200 µM of uranyl either in the nutrient solution or in water at pH 4.5. In these conditions, U was expected to be predominantly present as insoluble $(UO_2)_3(PO_4)_2$ in the nutrient solution and as soluble UO_2^{2+} in water. Plant shoot phenotypes are shown after 2 and 4 days of exposure to uranyl nitrate (Fig. 2A & B). The total

chlorophyll content was unchanged by U treatment (Fig. 2C), but anthocyanization of leaves was observed to correlate with exposure time and concentration for uranyl in water (Fig. 2D). Anthocyanization was particularly intense after 2 and 4 days of treatment with 200 µM U, and after 4 days of treatment with 50 µM U (Fig. 2B and D). In contrast, when U was supplied in culture medium, the anthocyanin content of plant leaves remained very low (Fig. 2B and 2D). These results indicate that plant stress was greater when plants were exposed to uranyl in water rather than in nutrient solution, most likely this is due to a higher U bioavailability in water (Fig. 1 and 2).

Kinetics of transcriptomic changes in response to uranyl exposure

To investigate the early response of Arabidopsis plants to U exposure, 7-week-old plants were treated with 50 µM uranyl nitrate in water and harvested after 2, 6 and 30 h. The Arabidopsis response was then analyzed on a genome-wide scale using CATMA microarrays (see Materials and Methods). The numbers of differentially expressed genes were: 1061 genes were up- or down-regulated after 2 h of treatment with 50 µM uranyl nitrate, while 256 and 823 genes were differentially expressed after 6 and 30 h of treatment, respectively (supplemental Figure S1). Among these differentially expressed genes, 111 were up- or down-regulated at all 3 timepoints (50 were up-regulated and 61 were down-regulated) (Supplemental Table S2: 'data.111' and 'integration' tabs, and Figure S2). We focused our subsequent analysis on this subset of genes. To gain insight into the biological processes in which the differentially expressed genes are involved, functional categorization was performed using the functional catalogue (FunCat).[37] Supplemental Table S2 ('FunCat.output' tab) summarizes the functional categories which were particularly affected by uranyl treatment. Categories with a P-value < 0.01 were retained for further investigation. The "Cell rescue, defense and virulence" category (23 genes in Supplemental Table S2) includes genes involved in 'Oxidative stress response', in 'Oxygen and radical detoxification' and in 'Disease, virulence and defense'. The "Interaction with the environment" category (18 genes) contains genes involved in 'Cellular sensing and response to external stimulus' and in 'Homeostasis'. The 'Cell wall' category and the "Systemic interaction with the environment" functional category, including 'Response to wounding', 'Immune response', 'Systemic acquired resistance' and 'Animal systemic sensing and response', were also well represented.

Real-time quantitative RT-PCR results confirm and complete CATMA microarray results

To validate the expression changes observed with CATMA microarrays, real-time quantitative RT-PCR analyses (qRT-PCR) were performed on five genes (three up- and two down-regulated)

selected from the 'Metabolism', 'Cellular transport, transport facilities and transport routes' and 'Interaction with the environment' categories. These genes code for the UDP-glucosyl transferase 73B4 (*UGT73B4*; AT2G15490), a purple acid phosphatase (*PAP17*; AT3G17790), a MATE efflux family protein (AT1G33110), a sodium:solute symporter family protein (urea transmembrane transporter; *DUR3*; AT5G45380), and a member of the high-affinity nitrate transporter family (*NRT2.5*; AT1G12940). Seven-week-old plants were treated with 0 and 50 µM uranyl nitrate for 2, 6, 30 and 48 h, and RNA was extracted from roots for qRT-PCR analyses (Figure 3). In the presence of 50 µM uranyl, *UGTT73B4*, *PAP17* and *MATE* were all up-regulated compared to the control (expression level ratios at t = 48 h: 8.5, 4.1 and 4.5, respectively). The two transporters, *DUR3* and *NRT2.5*, were down-regulated compared to the control, with a more pronounced response at 30 and 48 h (expression level ratios at t = 48 h: 0.09 and 0.02, respectively). Thus, overall, qRT-PCR and microarray analyses gave similar results, validating our transcriptomic approach.

As U was provided in water, and gene expression over time was compared with gene expression at t = 0, the trend for modulation of the expression of all the genes in the presence of water alone was also examined. *UGTT73B4* and *MATE* were down-regulated in plants grown in water alone, whereas *PAP17*, *DUR3* and *NRT2.5* were up-regulated in these conditions. Thus, the effects observed with U exposure are specific.

Uranium down-regulates iron-starvation response genes

Two genes involved in the iron uptake machinery were identified among the 61 root genes down-regulated at 2, 6 and 30 h of treatment with 50 µM uranyl nitrate. These were: *Ferric Reduction Oxidase2* (*FRO2*, AT1G01580), which codes for an epidermal ferric-chelate reductase involved in reducing Fe^{3+} to Fe^{2+};[38] and *Iron Regulated Transporter1* (*IRT1*, AT4G19690), which codes for the high-affinity Fe^{2+} transporter (supplemental Table S3). IRT1 controls the major route of Fe^{2+} entry in strategy I plants, which include *Arabidopsis thaliana*.[39-41] qRT-PCR experiments (Fig. 4A) confirmed the down-regulation of *FRO2* and *IRT1* in plants exposed to 50 µM uranyl, with relative expression level ratios of 0.005 and 0.014 for *FRO2* and *IRT1*, respectively, at 48 h.

In the CATMA microarray at 2 and 30 h of uranyl exposure, expression of *FIT1* (AT2G28160) was also down-regulated (with a P-value <0.001; at 6 h the down-regulation was significant with a P-value < 0.05) (supplemental Table S3); this was confirmed by qRT-PCR. *FIT1* codes for the basic helix-loop-helix FER-Like Fe-deficiency induced transcription factor1 (FIT1, FRU, BHLH039),[42-45] which positively regulates the expression of *FRO2* and *IRT1*. The expression profile of *FIT1* was similar to those of *IRT1* and *FRO2*, with strong down-regulation after 2 h of metal exposure which

increased over time to reach an expression level ratio of 0.034 at t = 48 h (Fig. 4A). Under iron starvation conditions, *Arabidopsis thaliana* responds by attempting to increase iron mobilization through the expression of two plasma membrane proton ATPases: AHA2 (AT4G30190) and AHA7 (AT3G60330). AHA2 mediates acidification of the rhizosphere; and *AHA7* expression is found to be strictly co-regulated with *IRT1* and *FRO2*. *AHA7* appears to be associated with the development of root hairs, the formation of which increases in response to iron deficiency.[46] Interestingly, both these major Fe-responsive H^+ ATPases were also down-regulated in response to uranyl, with an expression level ratio reaching 0.25 and 0.09 at 48 h of exposure for *AHA2* and *AHA7*, respectively (Fig. 4A).

The expression of three other genes involved in metal homeostasis was also disrupted by uranyl. The 'ZRT, IRT-like Protein' (ZIP3) transporter (AT2G32270), up-regulated in response to zinc deficiency and involved in zinc transport,[47,48] and Natural Resistance-Associated Macrophage Protein 1 (NRAMP1, AT1G80830), involved in iron and manganese transport,[49,50] were down-regulated at 2 and 30 h in the microarray experiment. The copper chaperone (CCH, AT3G56240) that participates in intracellular copper homeostasis[51] was up-regulated at 30 h. These gene expression trends were confirmed by qRT-PCR (Fig. 4B).

IRT1, *FRO2* and *FIT1* expression is modulated by uranium speciation

As U speciation plays an important role in its bioavailability, translocation and distribution in plants,[52,53] and it has been shown that the presence of phosphate reduces U bioavailability,[11,52,54] we also assessed gene expression for *IRT1*, *FRO2* and *FIT1* in roots of 7-week-old *Arabidopsis thaliana* plants treated with U (0, 5 and 50 µM) for 48 h in different conditions: in water, in water with 200 µM citrate, and in a depleted nutrient solution (without phosphate and EDTA). qRT-PCR data for these experiments are presented in Figure 5. As above, with 50 µM U in water, a strong down-regulation of *IRT1*, *FRO2* and *FIT1* was observed. These genes were also down-regulated at 5 µM U. The stronger reduction in expression observed at 50 µM corresponds to higher U levels accumulated in the roots (Fig. 6A). When plants were exposed to uranyl in complex with citrate, down-regulation of iron-starvation response genes was less pronounced. In these exposure conditions, the U content in roots is reduced and, as previously described,[52,55-57] at 50 µM U, citrate dramatically increases U translocation to the shoots (Fig. 6A). When U is supplied in EDTA- and phosphate-free culture medium, as in water, expression of the iron-starvation response genes is strongly reduced, especially at 50 µM U (Fig. 5). U content in the roots is also high in these conditions (Fig. 6A). Interestingly, iron content analysis shows that treatment with U does not affect the iron concentration found in roots and shoots (Fig. 6B). In roots, iron concentration is affected by

culture medium conditions (i.e. water vs. citrate vs. depleted culture medium) but not by uranyl concentration. When iron was present in the culture medium its concentration increased in plants, whereas the presence of citrate (which can chelate iron) caused a decrease in root concentration (Fig. 6B). Altogether, these results clearly show that the decreased *IRT1, FRO2* and *FIT1* expression in roots correlates with the uranyl concentration in the culture medium and its bioavailability.

Co-expression analysis of a large *Arabidopsis thaliana* microarray compendium gives new insights into the iron regulatory network and how it is affected by uranium

To further our understanding of the response induced in plants by U, we performed large-scale co-expression analysis using a compendium of microarrays composed of 1567 hybridized samples including different experimental conditions. We used a guide-gene approach to analyze these data.[35,58] This approach relies on the pre-selection of a set of genes known to be deregulated in a chosen condition or strongly linked to a biological process, and is mainly used to reveal genes of unknown, or poorly understood, function that could be implicated in the same pathways. We used the three U- and Fe-responsive genes (*IRT1*, *FRO2* and *FIT1*) as guide genes in our analysis. Co-expressed genes were grouped into modules using graphical representation of the microarray compendium where a node is a gene and the edge between two nodes indicates a similar expression profile within a subset of conditions. We used a compendium composed of CATMA two-color microarrays as source data.[59] Unlike ATH1 GeneChips, which are widely used for large-scale co-expression analysis, CATMA contains probes for *FIT1* and *FRO2*, making this system particularly appropriate for our study. We used a guide-gene strategy with three guide genes (*IRT1*, *FRO2* and *FIT1*) to reveal regulatory networks from the transcriptional profiles. Our approach differs slightly from popular co-expression strategies as it does not use the Pearson coefficient correlation to identify co-expression. The Pearson coefficient has been shown to be sensitive to outliers.[60] We also improved the way the co-expression graph was built to consider each microarray experiment (i.e., project) independently (see Materials and Methods). This overcomes potential bias due to experiments with large sample sizes. The resulting co-expression graph was composed of 19 genes (Fig. 7). Most of the conditions supporting the edges of a module were generally related to biotic and abiotic stresses, and to a lesser extent to characterization of Arabidopsis mutants (presented in supplemental Table S4). Among the genes present in the module co-expressing with *FIT1*, *IRT1* and *FRO2* (Supplemental Table S5), we identified the following genes coding for: APS reductase 1 (*APR1*) (involved in sulfur assimilation), an anti-oxidant 6-phosphogluconate dehydrogenase protein (part of the pentose phosphate pathway involved in the production of NADPH), a 2-oxoglutarate (2OG) and Fe(II)-dependent oxygenase, an important enzyme implicated

in the biosynthesis of plant secondary metabolites, a glutathione S-transferase (*GSTL1*), a methyl transferase (OMT1) also involved in secondary metabolism, two cellulose synthases (*CESA1* and *CESA3*) involved in cell wall formation. Finally, the proteins of unknown function included two membrane proteins - ABCB19, an ABC transporter also known as MDR11 (multi-drug resistance), and AT5G42090. When gene expression for all 19 genes (presented in Fig. 7) was analyzed in the U stress CATMA experiments, all these genes were found to be deregulated by U exposure. This confirms the overall effect of U on the expression of genes co-expressed with the genes involved in iron assimilation and homeostasis.

Discussion

This article presents an extensive molecular study of the effects of exposure to uranium on *Arabidopsis thaliana*, revealing involvement of unexpected gene pathways.

U speciation modeling, using J-Chess software, indicated that uranium (U) bioavalability would be greater in water than in culture medium. This was confirmed by measuring anthocyanin levels in *Arabidopsis thaliana* leaves following U exposure in either water or culture medium. The genome-wide transcriptome profile for hydroponically cultured plants exposed to 50 µM uranyl in water revealed a set of 111 genes whose expression profiles were altered at the three times examined. The transcriptome data for 13 genes were confirmed by qRT-PCR, indicating the reliability of our results. The 111 U-responsive genes were assigned to functional categories defined by FunCat (Supplemental Tables S2). This classification highlights specific cellular functions deregulated by U stress.

An overview of the functional gene categories deregulated early during U exposure

Our work reveals that exposure to U provokes a number of stress responses in roots, including a response to oxidative stress with alterations to the expression of 8 peroxidases. One of these, PRX52, located in the apoplast, was strongly induced by U in our analysis. This gene has been reported to be up-regulated in response to oxidative stress and fungal infection and is probably part of the general Arabidopsis defense system.[61] The other 7 peroxidases - also involved in the response to oxidative stress and for the majority located in the endomembrane system - were down-regulated. Thus, it appears that treatment with 50 µM uranyl nitrate for 30 h is perceived as an oxidative stress by the plant. Other authors have also indicated that the cellular redox balance may be disrupted by exposure to uranium.[7,8,10] Interestingly, at 30 h, U caused up-regulation of several genes coding for defense enzymes involved in ROS scavenging, including iron superoxide dismutase (*FSD1*),

catalase (*CAT3*), and several glutathione S-transferases (*GSTTU5*, *GSTTU6*, *GSTTU7*, *GSTTU19* and *GSTF2*) (data non shown). Exposure to uranyl also induced expression of the gene coding for lipoxygenase 3 (*LOX3*) - involved in the plant defense response - at all the times tested (2, 6 and 30 h); *LOX4* was also up-regulated at 2- and 30-h. *LOX1* has also been shown to be induced by U, but only from 100 μM.[10] In plants, LOX-derived fatty acid hydroperoxides can be further metabolized into volatile aldehydes and jasmonates, which play an important role as signaling molecules.[62]

Uranyl also induced the up-regulation of genes coding for proteins involved in the biosynthesis of salicylic acid (SA) and phytohormones implicated in the activation of plant defense responses against abiotic and biotic stress.[63] Among the phytohormones, the gene coding for isochorismate synthase 1 (*ICS1*) was strongly induced. This gene is usually up-regulated following pathogenic infection and stimulates SA synthesis. Interestingly, this up-regulation correlated with a strong induction of 9 transcription factor genes, including five members of the WRKY transcription factor family (*WRKY46*, *48*, *51*, *66* & *70*). These genes function as either positive or negative regulators of basal disease resistance in plants. For example, WRKY70 influences both plant senescence and defense signaling pathways[64] and functions as an activator of SA-dependent defense genes and a repressor of JA-regulated genes; WRKY48 is a stress- and pathogen-induced transcriptional activator that represses plant basal defense.[65] The NPR1-like protein 3 (NPR3), which was recently shown to be the receptor for the immune signal SA[66], was also induced at the three times in our study.

Some genes coding for kinases involved in protein phosphorylation were up-regulated by U, including PINOID serine/threonine kinase (*PID*). PID phosphorylates the PIN auxin efflux carriers[67] and, with PP2A phosphatase,[68] modulates the efflux of cellular auxin by modifying the polarity of the PIN transporters located in the plasma membrane. The increased expression of PINOID kinase induced by U will probably result in predominantly apical PIN targeting, leading to decreased auxin flow to the root tips.[69] This could explain some of the modifications to root morphology observed when plants are treated with U.

As with other heavy metals, the cell wall is the first structure directly exposed to U. Scanning electron micrographs of root cross sections showed precipitates containing uranyl adsorbed on cell walls in both the parenchymal and vascular root regions.[52] Our data show that U treatment led to down-regulation of genes involved in cell wall metabolism. These genes code for proteins which are essential for assembly and extension of the cell wall and for cell growth. They include 7 extensins or extensin-like family proteins, 2 expansins or genes involved in cell wall modification and the methylesterase PCR A.[70] [71] Genes involved in the synthesis of lignins - major components of the secondary cell walls - were also down-regulated, including the genes coding for cinnamyl-alcohol dehydrogenase (*CAD-C*) (down-regulated at all 3 timepoints) and

cinnamoyl-CoA-reductase (*CCR1*). *CAD-C* and *CCR1* are two of the main enzymes involved in constitutive lignification in *Arabidopsis thaliana*.[72,73] Genes involved in cell wall biosynthesis and plant growth were also deregulated when plants were challenged with U for a longer period (data not shown).

U stress alters expression of genes involved in phosphate homeostasis

Among the 111 genes whose expression was deregulated by U, *Purple Acid Phosphatase 17* (*PAP17*, *AtACP5*, AT3G17790) was up-regulated at the three timepoints in the microarray experiments. This up-regulation was confirmed by qRT-PCR. Interestingly, *PAP17* was shown to be strongly induced by phosphate starvation and also by oxidative stress.[74,75] We therefore searched for other phosphatase genes affected by U and found that the genes coding for Purple Acid Phosphatases 21 (*PAP21*, AT3G52810) and 22 (*PAP22*, AT3G52820) were also up-regulated at 30 h of U treatment (Supplemental Table S3). The gene coding for pyrophosphate-specific phosphatase1 (*PPsPase1*, AT1G73010) - recently identified and characterized as an inorganic pyrophosphatase-[76] was also found to be up-regulated at 2- and 30-h of U exposure. Another phosphate starvation-induced hydrolase gene, coding for a phosphoethanolamine / phosphocholine phosphatase 1(*PECP1*, AT1G17710),[77] was induced at 30 h of U exposure. Some other important components of the phosphate response, including the transcription factor PHR1 gene, were also deregulated by U genes (with a P-value < 0.05; supplemental Table S3). These results suggest that U stress deregulates phosphate sensing, triggering a phosphate starvation stress response and deregulation of the corresponding genes. This is probably due to the high affinity of U for phosphate, since synchrotron X-ray absorption spectroscopy and electron microscopy combined with energy dispersive spectroscopy showed that U speciation in plants involves complexes with endogenous phosphate, leading to its precipitation.[53,54,78] Thus, the phosphate becomes less available for plant metabolism, leading to a cellular response to starvation. Anthocyanization of the leaves upon exposure to uranyl could be correlated with the U-induced phosphate starvation since it is known that phosphate deprivation leads to anthocyanization.[79]

Uranyl perturbs root signaling and iron-uptake response leading to down-regulation of *FIT1*, *FRO2*, *IRT1*, *AHA2* and *AHA7*

Among the seven transporter genes deregulated by all uranyl treatments, we focused on the *IRT1* iron transporter gene since its down-regulation correlated with the down-regulation of the Fe^{3+} reductase gene, *FRO2*, which is also involved in iron uptake. The detailed qRT-PCR study of the

genes involved in iron assimilation and regulation showed that uranyl triggered a root iron-excess response resulting in down-regulation of *FIT1*, *FRO2*, *IRT1*, *AHA2* and *AHA7* (Fig. 4A). ICP-MS analysis of U concentrations showed that this response was dose-dependent (Fig. 6A). This response also depended on U speciation: when U was present in a citrate complex rather than as soluble uranyl, concentrations were lower in the roots and higher in the shoots. This confirms the importance of U speciation for its transfer, accumulation and translocation in plants.[52] ICP-MS analysis of iron content for plants exposed to U in water or citrate showed that U stress has a relatively low impact on plant iron redistribution in our experimental conditions (short term period). This suggests that the intensity of the effect on root iron induced by U was a direct result of the presence of U, rather than reflecting iron excess. When U treatment was performed in culture medium (in the presence of 20 µM $FeSO_4$ and without phosphate), *FIT1*, *FRO2* and *IRT1* were again down-regulated. The nutrient condition used in this experiment (presence of iron in the absence of phosphate) normally favors iron absorption by the roots, leading to a decrease in the expression of genes involved in iron homeostasis such *IRT1*.[75,80] Higher iron absorption is observed in all our expriments (Fig 6B), and U amplifies the phenomenon by triggering down-regulation of the iron-response genes. In contrast with results for *Arabidopsis halleri*,[81] our data reveal no increase in leaf iron content when uranyl was added to the culture medium. This apparent discrepancy is probably due to differences in plant culture conditions, in U exposure times and in medium composition between these two sets of experiments.

To further investigate the underlying molecular relationship between root iron and uranyl response, we performed co-expression analysis with *FIT1*, *FRO2* and *IRT1* as guide genes using a compendium of CATMA two-color microarrays as input data. This resource has been benchmarked and found to be a mature and valuable resource.[59] The Affymetrix ATH1 GeneChips, which are widely used in co-expression tools and databases, do not contain probes for *FRO2* and *FIT1*, making them unsuitable for our purposes. The CATMA microarray also potentially contains complementary information since it has not previously been used for co-expression studies. All the genes in the *FIT1*, *FRO2* and *IRT1*-associated transcriptional module had a down-regulated expression profile over the three timepoints studied, suggesting that transcription of these genes is co-regulated when plants are treated with U. Among the co-expressed genes, we particularly noticed AT5G02780 (*GSLT1*) and AT3G13610 (Oxidoreductase, 2OG-Fe(II) oxygenase family protein). Transcriptional profiling experiments using ATH1 GeneChips[82] revealed these genes to be differentially expressed in conditions leading to Fe deficiency in roots. Indeed, these two genes are thought to be regulated by the FIT1 transcription factor.[42] This suggests interplay between the iron signaling pathway and the uranyl transcriptional response involving these molecular actors. Co-expression approaches have been shown to yield biologically relevant information (for review

see.[35,60] Therefore, these results might be of interest in identifying candidates for further functional analysis as part of a more precise dissection of the underlying transcriptional network elicited by U conditions.

How can this effect on signaling and iron-uptake response be explained?

Our hypotheses explaining how U perturbs root signaling and iron-uptake response at the cellular level are summarized in Figure 8. First, uranyl, which is a hard Lewis acid, could displace iron (III), also a hard Lewis acid, from proteins containing iron or other ligands such as phosphate, thus triggering an increase in free iron within the cell. This excess iron would be perceived via the iron signaling pathway, leading to down- regulation of *FIT1* followed by down-regulation of the expression of the other genes involved in iron assimilation. Iron release within the cell could result in oxidative stress, as observed when plants are treated with U, since free iron induces the production of reactive oxygen species through the Fenton reaction. An excess of cellular iron would trigger increased ferritin expression, and U effectively up-regulated *Fer3* expression (at 30 h, P-value <0.05; supplemental Table S3). However, *Fer1* was not affected. Recently, Bournier et al[83] revealed a direct molecular link between iron and phosphate homeostasis, showing that PHR1 regulates *Fer1* expression in an iron-independent manner. Thus, here the down regulation of *PHR1* by U could explain the loss of *Fer1* expression and may be the reason for U toxicity. An alternative, not necessarily mutually exclusive, hypothesis would be that a high U content is perceived as an excess of iron (III) either via the unknown cellular iron sensor[84] or by interacting with cellular component involved in iron signaling. This hypothesis is supported by the fact that, in humans, uranyl can replace iron (III) in some proteins including serum transferrin - which is involved in iron transport.[85] Uranyl-loaded transferrin could then interact with the transferrin receptor 1-mediated iron-acquisition pathway.[86] In support of this, plutonium, which is also an actinide, was recently shown to be absorbed by rat adrenal gland cells via the same iron-acquisition pathway.[87] Because of the strong effect of uranyl on the iron regulatory network, a metallomic approach is currently being undertaken in our laboratory to identify uranyl-binding proteins and to characterize new molecular actors potentially involved in regulating iron homeostasis in plants.

References

1. F. Paquet, C. Adam-Guillermin, E. Ansoborlo, K. Beaugelin-Seiller, M. Carrière, I. Dublineau, F. Taran, C. Vidaud In *Toxicologie nucléaire environnementale et humaine*; Lavoisier, 2009, p 411.
2. H. Vandenhove, *Int. Congr. Ser.,* 2002, 307.

3. L. A. Schipper, G. P. Sparling, L. M. Fisk, M. B. Dodd, I. L. Power, R. A. Littler, *Agriculture Ecosystems & Environment,* 2011, **144**, 95.

4. J. Wetterlind, A. C. Richer De Forges, B. Nicoullaud, D. Arrouays, *Soil Use and Management,* 2012, **28**, 101.

5. S. C. Sheppard, M. I. Sheppard, M. O. Gallerand, B. Sanipelli, *J. Environ. Radioactiv.,* 2005, **79**, 55.

6. D. Ribera, F. Labrot, G. Tisnerat, J. F. Narbonne, *Rev. Environ. Contam. Toxicol.,* 1996, **146**, 53.

7. H. Vandenhove, A. Cuypers, M. Van Hees, G. Koppen, J. Wannijn, *Plant Physiol. Biochem.,* 2006, **44**, 795.

8. N. Vanhoudt, A. Cuypers, N. Horemans, T. Remans, K. Opdenakker, K. Smeets, D. M. Bello, M. Havaux, J. Wannijn, M. Van Hees, J. Vangronsveld, H. Vandenhove, *J. Environ. Radioactiv.,* 2011, **102**, 638.

9. N. Vanhoudt, H. Vandenhove, N. Horemans, D. M. Bello, M. Van Hees, J. Wannijn, R. Carleer, J. Vangronsveld, A. Cuypers, *J. Plant Nutr.,* 2011, **34**, 1940.

10. N. Vanhoudt, H. Vandenhove, N. Horemans, T. Remans, K. Opdenakker, K. Smeets, D. M. Bello, J. Wannijn, M. Van Hees, J. Vangronsveld, A. Cuypers, *J. Environ. Radioactiv.,* 2011, **102**, 630.

11. N. Vanhoudt, H. Vandenhove, K. Smeets, T. Remans, M. Van Hees, J. Wannijn, J. Vangronsveld, A. Cuypers, *Plant Physiol. Biochem.,* 2008, **46**, 987.

12. K. Viehweger, G. Geipel, G. Bernhard, *Biometals,* 2011, **24**, 1197.

13. M. Becher, I. N. Talke, L. Krall, U. Kramer, *Plant J.,* 2004, **37**, 251.

14. M. Weber, E. Harada, C. Vess, E. von Roepenack-Lahaye, S. Clemens, *Plant J.,* 2004, **37**, 269.

15. M. Weber, A. Trampczynska, S. Clemens, *Plant Cell Environ.,* 2006, **29**, 950.

16. S. Herbette, L. Taconnat, V. Hugouvieux, L. Piette, M. L. M. Magniette, S. Cuine, P. Auroy, P. Richaud, C. Forestier, J. Bourguignon, J. P. Renou, A. Vavasseur, N. Leonhardt, *Biochimie,* 2006, **88**, 1751.

17. J. E. Sarry, L. Kuhn, C. Ducruix, A. Lafaye, C. Junot, V. Hugouvieux, A. Jourdain, O. Bastien, J. B. Fievet, D. Vailhen, B. Amekraz, C. Moulin, E. Ezan, J. Garin, J. Bourguignon, *Proteomics,* 2006, **6**, 2180.

18. F. Villiers, C. Ducruix, V. Hugouvieux, N. Jarno, E. Ezan, J. Garin, C. Junot, J. Bourguignon, *Proteomics,* 2011, **11**, 1650.

19. P. Le Lay, M. P. Isaure, J. E. Sarry, L. Kuhn, B. Fayard, J. L. Le Bail, O. Bastien, J. Garin, C. Roby, J. Bourguignon, *Biochimie,* 2006, **88**, 1533.

20. M. L. Crowe, C. Serizet, V. Thareau, S. Aubourg, P. Rouze, P. Hilson, J. Beynon, P. Weisbeek, P. van Hummelen, P. Reymond, J. Paz-Ares, W. Nietfeld, M. Trick, *Nucleic Acids Res.,* 2003, **31**,

156.

21. P. Hilson, I. Small, M. T. R. Kuiper, *Curr. Opin. Plant Biol.,* 2003, **6**, 426.
22. M. L. Martin-Magniette, J. Aubert, E. Cabannes, J. J. Daudin, *Bioinformatics,* 2005, **21**, 1995.
23. S. Lemoine, F. Combes, N. Servant, S. Le Crom, *BMC Bioinformatics,* 2006, **7**, 467.
24. G. K. Smyth In *Bioinformatics and Computational Biology Solutions using R and Bioconductor*; Springer, New York, 2005, p 397.
25. R. C. Gentleman, V. J. Carey, D. M. Bates, B. Bolstad, M. Dettling, S. Dudoit, B. Ellis, L. Gautier, Y. C. Ge, J. Gentry, K. Hornik, T. Hothorn, W. Huber, S. Iacus, R. Irizarry, F. Leisch, C. Li, M. Maechler, A. J. Rossini, G. Sawitzki, C. Smith, G. Smyth, L. Tierney, J. Y. H. Yang, J. H. Zhang, *Genome Biology,* 2004, **5**, R80.
26. Y. Benjamini, Y. Hochberg, *J R Stat Soc Series B Stat Methodol,* 1995, **57**, 289.
27. K. J. Livak, T. D. Schmittgen, *Methods,* 2001, **25**, 402.
28. D. I. Arnon, *Plant Physiol.,* 1949, **24**, 1.
29. H. Lange, W. Shropshire, JR., H. Mohr, *Plant Physiol.,* 1971, **47**, 649.
30. L. Bion, *Radiochim. Acta,* 2003, **91**, 633.
31. F. H. Denison, J. Garnier-LaPlace, *Geochim Cosmochim AC,* 2005, **69**, 2183.
32. S. Gagnot, J. P. Tamby, M. L. Martin-Magniette, F. Bitton, L. Taconnat, S. Balzergue, S. Aubourg, J. P. Renou, A. Lecharny, V. Brunaud, *Nucleic Acids Res.,* 2008, **36**, D986.
33. G. K. Smyth, J. Michaud, H. S. Scott, *Bioinformatics,* 2005, **21**, 2067.
34. F. Boyer, F. Combes, J. Bourguignon, Y. A. Vandenbrouck In *Sixth International Workshop on Computational Systems Biology, WCSB 2009* Aarhus, Denmark, 2009, p 23.
35. K. Aoki, Y. Ogata, D. Shibata, *Plant Cell Physiol.,* 2007, **48**, 381.
36. J. Van der Lee, L. C. De Windt; Paris., U. M. L. R. E. d. M. d., Ed. Fontainebleau, France,, 2002.
37. A. Ruepp, A. Zollner, D. Maier, K. Albermann, J. Hani, M. Mokrejs, I. Tetko, U. Guldener, G. Mannhaupt, M. Munsterkotter, H. W. Mewes, *Nucleic Acids Res.,* 2004, **32**, 5539.
38. N. J. Robinson, C. M. Procter, E. L. Connolly, M. L. Guerinot, *Nature,* 1999, **397**, 694.
39. D. Eide, M. Broderius, J. Fett, M. L. Guerinot, *Proc. Natl. Acad. Sci. U. S. A.,* 1996, **93**, 5624.
40. G. Vert, N. Grotz, F. Dedaldechamp, F. Gaymard, M. L. Guerinot, J. F. Briat, C. Curie, *Plant Cell,* 2002, **14**, 1223.
41. R. Henriques, J. Jasik, M. Klein, E. Martinoia, U. Feller, J. Schell, M. S. Pais, C. Koncz, *Plant Mol. Biol.,* 2002, **50**, 587.
42. E. P. Colangelo, M. L. Guerinot, *Plant Cell,* 2004, **16**, 3400.
43. H. Q. Ling, P. Bauer, Z. Bereczky, B. Keller, M. Ganal, *Proc. Natl. Acad. Sci. U. S. A.,* 2002, **99**, 13938.

44. M. Jakoby, H. Y. Wang, W. Reidt, B. Weisshaar, P. Bauer, *FEBS Lett.,* 2004, **577**, 528.
45. Y. X. Yuan, J. Zhang, D. W. Wang, H. Q. Ling, *Cell Res.,* 2005, **15**, 613.
46. S. Santi, W. Schmidt, *New Phytol.,* 2009, **183**, 1072.
47. N. Grotz, T. Fox, E. Connolly, W. Park, M. L. Guerinot, D. Eide, *Proc. Natl. Acad. Sci. U. S. A.,* 1998, **95**, 7220.
48. M. L. Guerinot, *BBA-Biomembranes,* 2000, **1465**, 190.
49. C. Curie, J. M. Alonso, M. Le Jean, J. R. Ecker, J. F. Briat, *Biochem. J.,* 2000, **347**, 749.
50. R. Cailliatte, A. Schikora, J. F. Briat, S. Mari, C. Curie, *Plant Cell,* 2010, **22**, 904.
51. L. J. Shin, J. C. Lo, K. C. Yeh, *Plant Physiol.,* 2012, **159**, 1099.
52. J. Laurette, C. Larue, C. Mariet, F. Brisset, H. Khodjad, J. Bourguignon, M. Carrière, *Environ. Exp. Bot.,* 2012, **77**, 96.
53. J. Laurette, C. Larue, I. Llorens, D. Jaillard, P. H. Jouneau, J. Bourguignon, M. Carrière, *Environ. Exp. Bot.,* 2012, **77**, 87.
54. J. Misson, P. Henner, M. Morello, M. Floriani, T. D. Wu, J. L. Guerquin-Kern, L. Fevrier, *Environ. Exp. Bot.,* 2009, **67**, 353.
55. J. Mihalik, P. Henner, S. Frelon, V. Camilleri, L. Fevrier, *Environ. Exp. Bot.,* 2012, **77**, 249.
56. J. Mihalik, P. Tlustos, J. Szakova, *Journal of Radioanalytical and Nuclear Chemistry,* 2010, **285**, 279.
57. S. D. Ebbs, D. J. Brady, L. V. Kochian, *J. Exp. Bot.,* 1998, **49**, 1183.
58. J. Lisso, D. Steinhauser, T. Altmann, J. Kopka, C. Mussig, *Nucleic Acids Res.,* 2005, **33**, 2685.
59. J. Allemeersch, S. Durinck, R. Vanderhaeghen, P. Alard, R. Maes, K. Seeuws, T. Bogaert, K. Coddens, K. Deschouwer, P. Van Hummelen, M. Vuylsteke, Y. Moreau, J. Kwekkeboom, A. H. M. Wijfjes, S. May, J. Beynon, P. Hilson, M. T. R. Kuiper, *Plant Physiol.,* 2005, **137**, 588.
60. B. Usadel, T. Obayashi, M. Mutwil, F. M. Giorgi, G. W. Bassel, M. Tanimoto, A. Chow, D. Steinhauser, S. Persson, N. J. Provart, *Plant Cell Environ.,* 2009, **32**, 1633.
61. S. Floerl, A. Majcherczyk, M. Possienke, K. Feussner, H. Tappe, C. Gatz, I. Feussner, U. Kues, A. Polle, *Plos One,* 2012, **7**, e31435.
62. A. Andreou, I. Feussner, *Phytochemistry,* 2009, **70**, 1504.
63. G. Loake, M. Grant, *Curr. Opin. Plant Biol.,* 2007, **10**, 466.
64. B. Ulker, M. S. Mukhtar, I. E. Somssich, *Planta,* 2007, **226**, 125.
65. D. H. Xing, Z. B. Lai, Z. Y. Zheng, K. M. Vinod, B. F. Fan, Z. X. Chen, *Molecular Plant,* 2008, **1**, 459.
66. Z. Q. Fu, S. P. Yan, A. Saleh, W. Wang, J. Ruble, N. Oka, R. Mohan, S. H. Spoel, Y. Tada, N. Zheng, X. N. Dong, *Nature,* 2012, **486**, 228.
67. J. Friml, X. Yang, M. Michniewicz, D. Weijers, A. Quint, O. Tietz, R. Benjamins, P. B. F.

Ouwerkerk, K. Ljung, G. Sandberg, P. J. J. Hooykaas, K. Palme, R. Offringa, *Science,* 2004, **306**, 862.

68. M. Michniewicz, M. K. Zago, L. Abas, D. Weijers, A. Schweighofer, I. Meskiene, M. G. Heisler, C. Ohno, J. Zhang, F. Huang, R. Schwab, D. Weigel, E. M. Meyerowitz, C. Luschnig, R. Offringa, J. Friml, *Cell,* 2007, **130**, 1044.
69. J. Zhang, T. Nodzynski, A. Pencik, J. Rolcik, J. Friml, *Proc. Natl. Acad. Sci. U. S. A.,* 2010, **107**, 918.
70. D. T. A. Lamport, M. J. Kieliszewski, Y. N. Chen, M. C. Cannon, *Plant Physiol.,* 2011, **156**, 11.
71. Y. Lee, D. Choi, H. Kende, *Curr. Opin. Plant Biol.,* 2001, **4**, 527.
72. T. Goujon, R. Sibout, A. Eudes, J. MacKay, L. Jouanin, *Plant Physiol. Biochem.,* 2003, **41**, 677.
73. R. Sibout, A. Eudes, G. Mouille, B. Pollet, C. Lapierre, L. Jouanin, A. Seguin, *Plant Cell,* 2005, **17**, 2059.
74. J. C. del Pozo, I. Allona, V. Rubio, A. Leyva, A. de la Pena, C. Aragoncillo, J. Paz-Ares, *Plant J.,* 1999, **19**, 579.
75. J. Misson, K. G. Raghothama, A. Jain, J. Jouhet, M. A. Block, R. Bligny, P. Ortet, A. Creff, S. Somerville, N. Rolland, P. Doumas, P. Nacry, L. Herrerra-Estrella, L. Nussaume, M. C. Thibaud, *Proc. Natl. Acad. Sci. U. S. A.,* 2005, **102**, 11934.
76. A. May, S. Berger, T. Hertel, M. Kock, *BBA-General Subjects,* 2011, **1810**, 178.
77. A. May, M. Spinka, M. Kock, *BBA-Proteins and Proteomics,* 2012, **1824**, 319.
78. A. Gunther, G. Bernhard, G. Geipel, T. Reich, A. Rossberg, H. Nitsche, *Radiochim. Acta,* 2003, **91**, 319.
79. K. G. Raghothama, *Annu. Rev. Plant Physiol. Plant Molec. Biol.,* 1999, **50**, 665.
80. J. Hirsch, E. Marin, M. Floriani, S. Chiarenza, P. Richaud, L. Nussaume, M. C. Thibaud, *Biochimie,* 2006, **88**, 1767.
81. K. Viehweger, G. Geipel, *Environ. Exp. Bot.,* 2010, **69**, 39.
82. T. J. W. Yang, W. D. Lin, W. Schmidt, *Plant Physiol.,* 2010, **152**, 2130.
83. M. Bournier, N. Tissot, S. Mari, J. Boucherez, E. Lacombe, J.-F. Briat, F. Gaymard, *J. Biol. Chem.,* 2013, **288**, 22670.
84. M. N. Hindt, M. L. Guerinot, *BBA-Molecular Cell Research,* 2012, **1823**, 1521.
85. C. Vidaud, S. Gourion-Arsiquaud, F. Rollin-Genetet, C. Torne-Celer, S. Plantevin, O. Pible, C. Berthomieu, E. Quemeneur, *Biochemistry (Mosc).* 2007, **46**, 2215.
86. M. Hemadi, N. T. Ha-Duong, S. Plantevin, C. Vidaud, J. M. E. Chahine, *J. Biol. Inorg. Chem.,* 2010, **15**, 497.
87. M. P. Jensen, D. Gorman-Lewis, B. Aryal, T. Paunesku, S. Vogt, P. G. Rickert, S. Seifert, B. Lai, G. E. Woloschak, L. Soderholm, *Nature Chem. Biol.,* 2011, **7**, 560.

Figure legends

Figure 1. Calculating U speciation. U speciation was modeled as a function of pH using J-Chess software and the BASSIST database, for 5, 50 and 200 µM uranyl nitrate in culture medium (A, B & C) and water (D, E & F). The details of culture medium composition are provided in the Materials and Methods section. Full lines correspond to soluble U species; broken lines are precipitated species.

Figure 2. Characterization of plants treated with uranyl nitrate in hydroponic conditions. Seven-week-old *Arabidopsis thaliana* plants were treated with 0, 50 and 200 µM uranyl nitrate in culture medium (A) or water at pH 4.5 (B) for 0, 2 and 4 days. Total chlorophyll (C) and anthocyanin (D) were determined in leaves from plants treated with the three concentrations of uranyl nitrate over the same time course. Three biological replicates were performed for each condition. Confidence intervals for the means were calculated at a 95% level.

Figure 3. Real-time quantitative RT-PCR validation of microarray data performed on 7 week-old plants treated with 0 or 50 µM of uranyl nitrate. Graphs show the kinetics of gene expression in Arabidopsis thaliana roots from plants treated with 0 or 50 µM uranyl nitrate at 2, 6, 30 and 48 h of exposure. Five genes selected in the CATMA chip, coding for a UDP-glucosyl transferase (*UGT73B4*, AT2G15490), a purple acid phosphatase (*PAP17*, AT3G17790), a MATE efflux family protein (*MATE*, AT1G33110), a sodium:solute symporter family protein (*DUR3*, AT5G45380), and a member of the high-affinity nitrate transporter family (*NRT2.5*, AT1G12940) were shown by microarray analysis to be differentially expressed in roots. These genes were further analyzed by real-time quantitative RT-PCR. All data are given relative to the control plant before treatment and are shown as mean ± S.D. of three replicates. The primers used in these experiments are listed in Supplemental Table S1.

Figure 4. Real-time quantitative RT-PCR validation of U effects on the expression of genes involved in iron assimilation and regulatory networks (A) and other metal homeostasis genes (B). Graphs show the kinetics of gene expression in *Arabidopsis thaliana* roots from 7 week-old plants treated with 0 or 50 µM uranyl nitrate at 2, 6, 30 and 48 h of exposure. (A) Down-regulation of ferric reductase oxidase2 (*FRO2*, AT1G01580), the high-affinity Fe^{2+} transporter (*IRT1*, AT4G19690), FIT1 transcription factor (AT2G28160), and two plasma membrane H^+ ATPase

(*AHA2*, AT4G30190 and *AHA7*, AT3G60330) expression confirmed by real-time quantitative RT-PCR. (B) Confirmation of the deregulated expression of genes coding for a member of the ZRT- and IRT- related Protein (*ZIP3*, AT2G32270), the Natural Resistance-Associated Macrophage Protein1 (*NRAMP1*, AT1G80830), and the Copper Chaperone (*CCH*, AT3G56240). All data are shown relative to the control plant before treatment; data points show mean ± S.D. for three replicates. The primers used in these experiments are listed in Supplemental Table S1.

Figure 5. Impact of uranium speciation on the expression of genes involved in iron assimilation and regulatory networks. Real-time quantitative RT-PCR experiments were performed on the roots of 7-week-old Arabidopsis plants exposed to 0, 5 or 50 µM uranyl nitrate for 48 h. Uranium was provided in water (pH 4.5), in water supplemented with citrate (200 µM, pH 4.5), or in EDTA- and phosphate-free culture medium. Expression levels for *IRT1*, *FRO2* and *FIT1* were determined for each exposure condition. Data points indicate mean ± SEM of three replicates.

Figure 6. Impact of uranium speciation on uranium and iron accumulation and distribution in *Arabidopsis thaliana* roots and shoots. ICP-MS was used to determine uranium (A) and iron (B) levels in the shoots and roots of 7-week-old Arabidopsis plants exposed to 0, 5 and 50 µM of uranyl nitrate for 48 h. Uranyl nitrate was supplied in water (pH 4.5) ('H_2O'), water supplemented with citrate (200 µM, pH 4.5) ('citrate'), or in EDTA- and phosphate-free culture medium. Results are mean ± SEM of three replicates.

Figure 7. Transcriptional module with *IRT1*, *FRO2* and *FIT1* as bait genes. Bait genes are represented by a square. Each node represents a gene, and each edge represents the co-expression relationship between two genes. The thickness of edges is determined by the number of CATMA projects supporting co-expression of a pair of genes (i.e., the thicker the edge, the more projects support co-expression). Histograms indicate the expression values obtained from CATMA microarray experiments at each time point. The transcriptional module was drawn and printed using Cytoscape software (v. 2.8 – http://www.cytoscape.org).

Figure 8. Summary of hypotheses explaining how uranyl perturbs signaling and iron-uptake response. FIT1: transcription factor regulating iron uptake responses; IRT1: iron high-affinity transporter; FRO2: ferric-chelate reductase and AHA2/7: plasma membrane H+ ATPases.

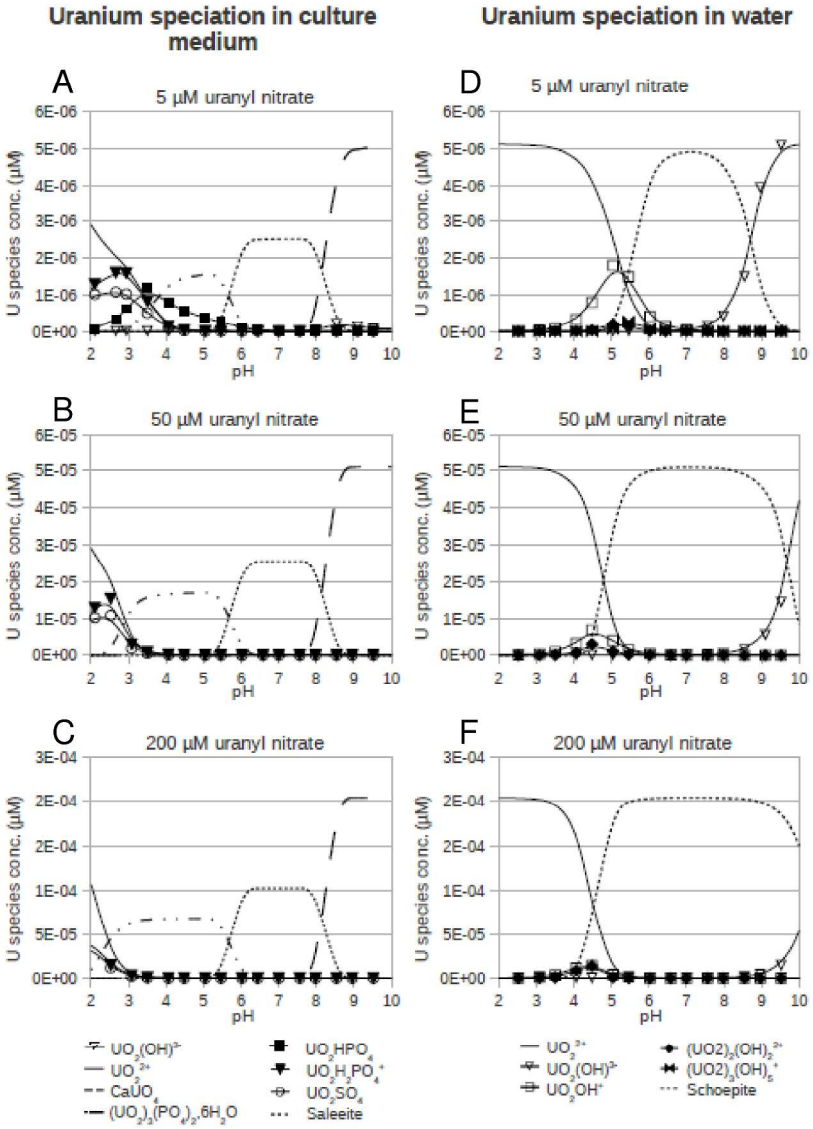

181x254mm (600 x 600 DPI)

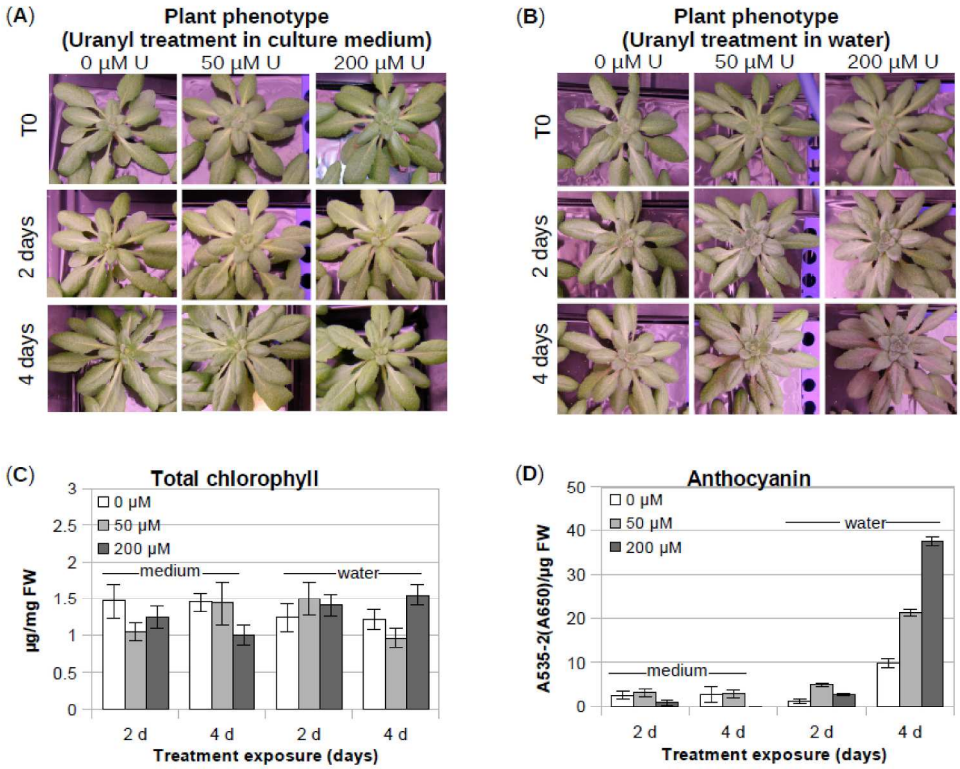

126x108mm (600 x 600 DPI)

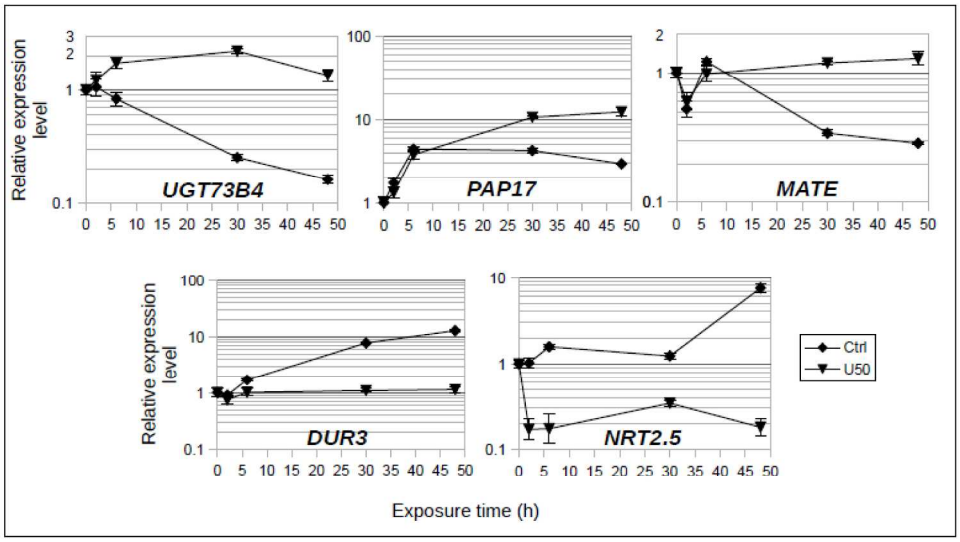

101x60mm (600 x 600 DPI)

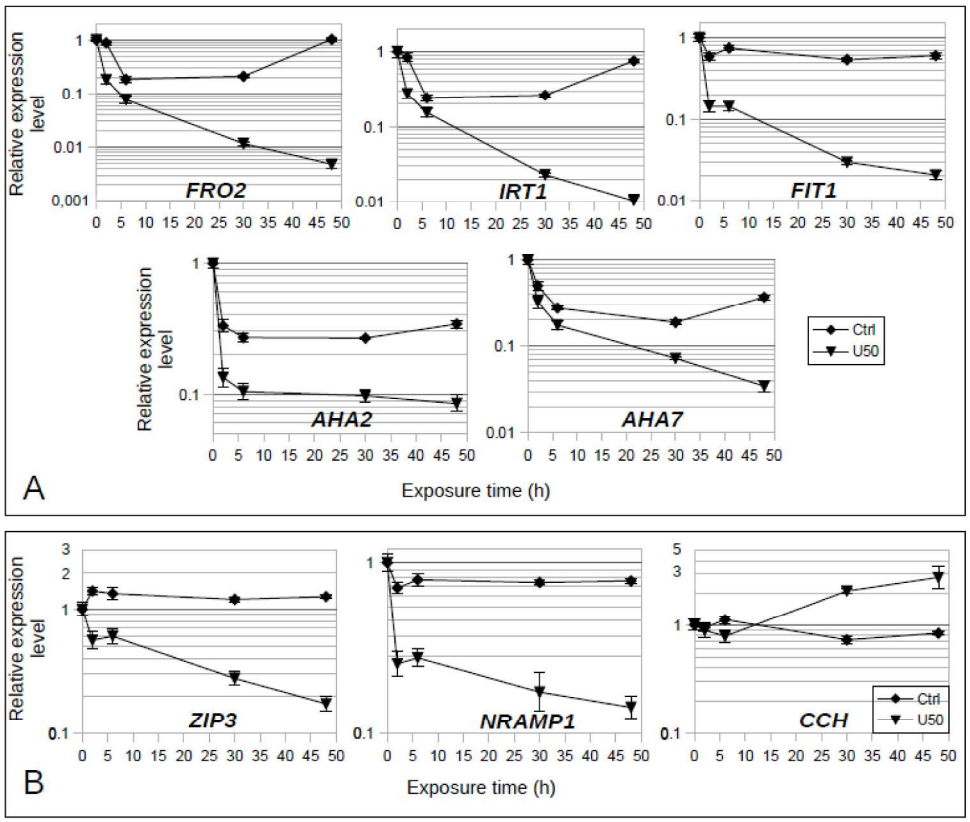

140x116mm (600 x 600 DPI)

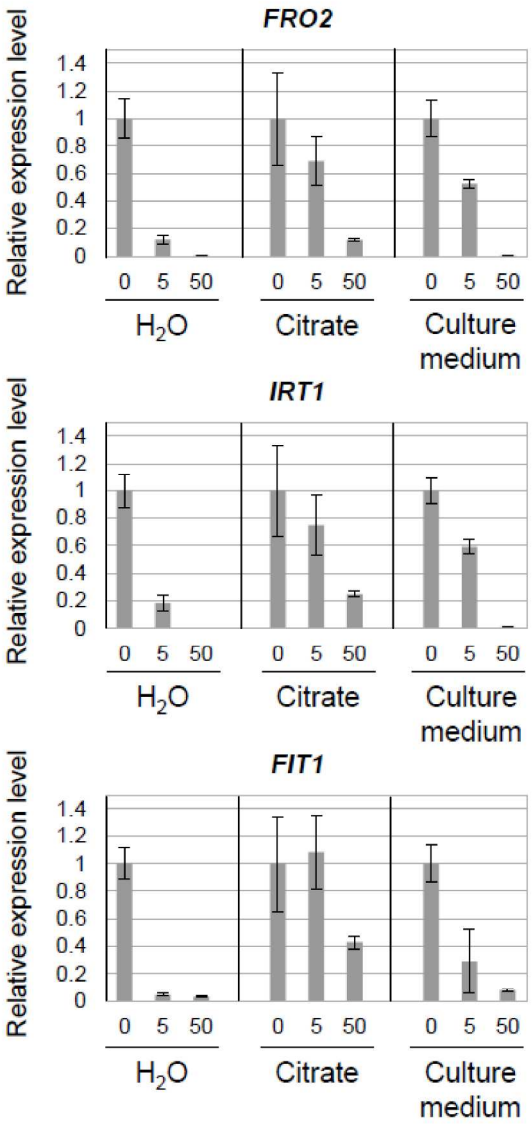

196x409mm (600 x 600 DPI)

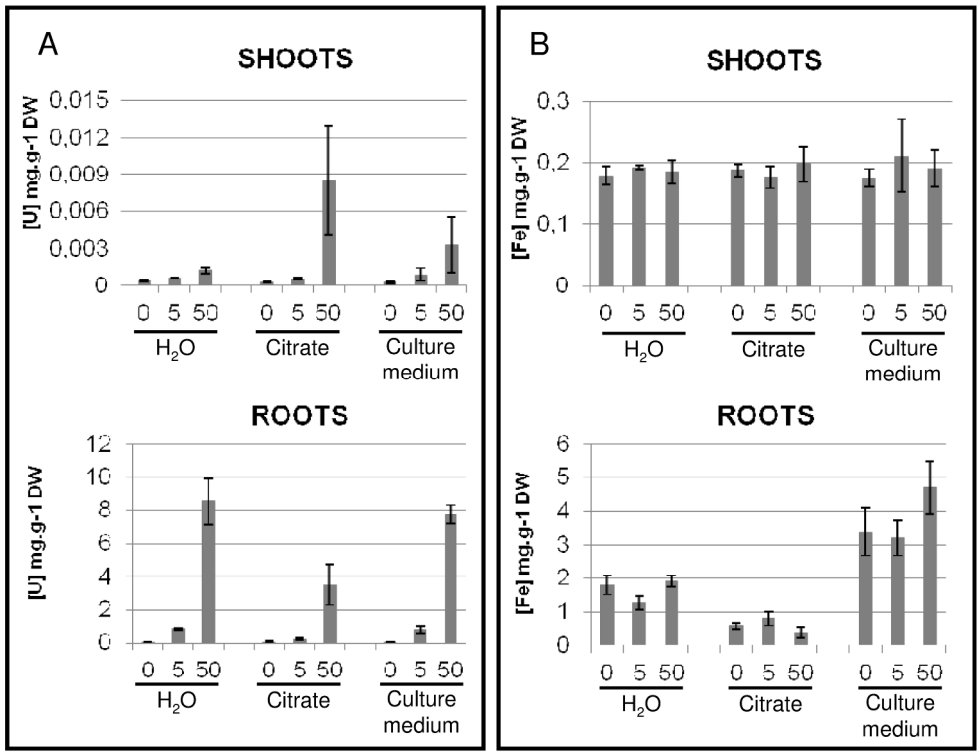

128x100mm (600 x 600 DPI)

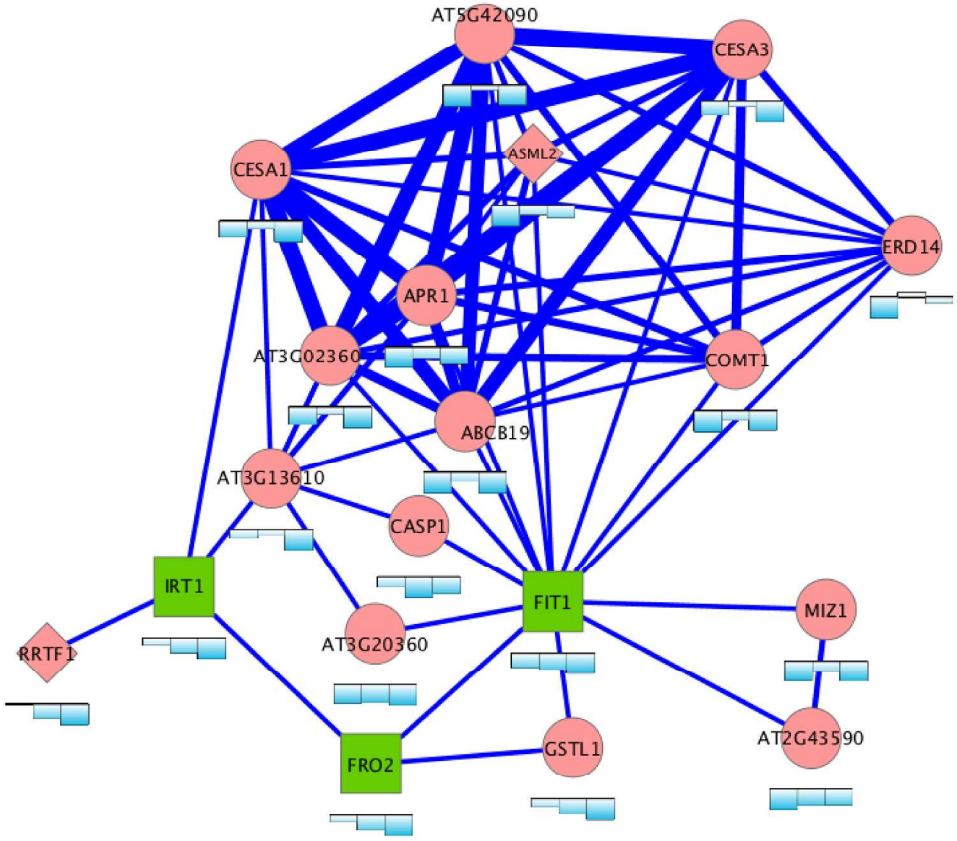

108x101mm (600 x 600 DPI)

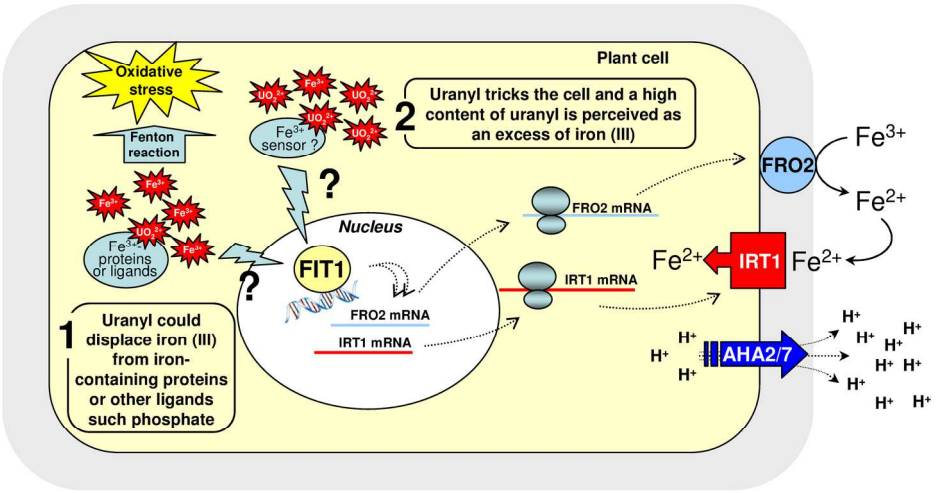

89x48mm (600 x 600 DPI)